doi:10.1016/j.jmb.2010.10.055 J. Mol. Biol. (2011) 405, 754–764

Contents lists available at www.sciencedirect.com

Journal of Molecular Biology

journal homepage: http://ees.elsevier.com.jmb

The RelA Nuclear Localization Signal Folds upon Binding to IκBα

Carla F. Cervantes[1], Simon Bergqvist[1], Magnus Kjaergaard[1], Gerard Kroon[2], Shih-Che Sue[3], H. Jane Dyson[2]* and Elizabeth A. Komives[1]*

[1]*Department of Chemistry and Biochemistry, University of California, San Diego, 9500 Gilman Drive, La Jolla, CA 92092-0378, USA*

[2]*Department of Molecular Biology, The Scripps Research Institute, 10550 North Torrey Pines Road, La Jolla, CA 92037, USA*

[3]*Institute of Bioinformatics and Structural Biology, National Tsing Hua University, 101 Sec 2, Kuang Fu Road, Hsinchu 30013, Taiwan*

Received 19 September 2010; received in revised form 27 October 2010; accepted 27 October 2010
Available online 19 November 2010

Edited by J. E. Ladbury

Keywords:
nuclear localization;
ankyrin repeat;
NMR;
intrinsically disordered protein;
coupled folding and binding

The nuclear localization signal (NLS) polypeptide of RelA, the canonical nuclear factor-κB family member, is responsible for regulating the nuclear localization of RelA-containing nuclear factor-κB dimers. The RelA NLS polypeptide also plays a crucial role in mediating the high affinity and specificity of the interaction of RelA-containing dimers with the inhibitor IκBα, forming two helical motifs according to the published X-ray crystal structure. In order to define the nature of the interaction between the RelA NLS and IκBα under solution conditions, we conducted NMR and isothermal titration calorimetry studies using a truncated form of IκBα containing residues 67–206 and a peptide spanning residues 293–321 of RelA. The NLS peptide, although largely unfolded, has a weak tendency toward helical structure when free in solution. Upon addition of the labeled peptide to unlabeled IκBα, the resonance dispersion in the NMR spectrum is significantly greater, providing definitive evidence that the RelA NLS polypeptide folds upon binding IκBα. Isothermal titration calorimetry studies of single-point mutants reveal that residue F309, which is located in the middle of the more C-terminal of the two helices (helix 4) in the IκBα-bound RelA NLS polypeptide, is critical for the binding of the RelA NLS polypeptide to IκBα. These results help to explain the role of helix 4 in mediating the high affinity of RelA for IκBα.

*Corresponding authors. E-mail address: ekomives@ucsd.edu.

Present addresses: C. F. Cervantes, Department of Molecular Biology, The Scripps Research Institute, 10550 North Torrey Pines Road, La Jolla CA 92037, USA; M. Kjaergaard, Department of Biology, University of Copenhagen, Ole Maaloes Vej 5, DK-2200 Copenhagen N, Denmark.

Abbreviations used: NLS, nuclear localization signal; ITC, isothermal titration calorimetry; HSQC, heteronuclear single quantum coherence; NOE, nuclear Overhauser enhancement; NFκB, nuclear factor κB.

Introduction

The nuclear factor κB (NFκB) family of transcription factors is a key component in the control of many cellular signaling events including cellular stress responses, cell growth, survival, and apoptosis.[1–3] The NFκB signaling system is activated by at least 58 viral or bacterial products, 46 stress conditions and chemicals, at least 32 cytokines and receptor ligands, as well as apoptotic mediators and mitogens, resulting in the transcription of more than 150 genes.[4] In resting cells, NFκB dimers are

0022-2836/$ - see front matter

sequestered in the cytoplasm *via* their interaction with proteins from the inhibitor of κB (IκB) family.[5] IκBα, the most abundant and best-characterized member of the IκB family, is capable of inhibiting many of the NFκB family members, including the most abundant, NFκB(RelA (also known as p65)/p50), and other RelA- and cRel-containing homo- and hetero-dimers.[6] The NFκB–IκBα complex is highly stable in resting cells, with a half-life of >12 h.[7] However, even a small amount of NFκB, which may be released due to leaky inhibition, would be sufficient to give gene expression; thus, a second tier of control, tight regulation of NFκB nuclear localization, is employed to ensure cell homeostasis.[7,8]

Regulation of nuclear localization of RelA occurs *via* its nuclear localization sequence (NLS), which targets it to the nucleus. Formation of the complex with IκBα sequesters RelA-containing NFκB in the cytoplasm by masking the RelA NLS within the binding interface.[9,10] Upon stimulation, IκBα is phosphorylated, ubiquitinated, and degraded, unmasking the RelA NLS and thus allowing its translocation to the nucleus and subsequent transcriptional activation activity. NLS sequences are generally short 3- to 20-amino-acid sequences with a consensus sequence, K-(K/R)-X-(K/R), which mediates nuclear import *via* recognition by the nuclear import receptor.[11–15] The sequence KRKR, found at residues 301–304 within the RelA NLS polypeptide (generally identified as residues 289–321), is located at the carboxyl terminus of the rel homology domain of RelA (Fig. 1a).[16]

The crystal structures of NFκB (RelA/p50) bound to IκBα reveal an extended protein–protein interface formed between IκBα and NFκB.[10,17] IκBα contacts NFκB *via* its six-ankyrin repeat domain and C-terminal PEST region, forming multiple contacts with the RelA NLS polypeptide; p50 and RelA dimerization domain; and amino-terminal domain regions that comprise NFκB(RelA/p50).[10,17] The two proteins run antiparallel, with ankyrin repeats 1–3 (AR1–3) contacting the RelA NLS polypeptide, which adopts a helix–turn–helix fold (Fig. 1b).[10] AR1 is capped by helix 4 of the RelA NLS polypeptide (residues 305–321) *via* hydrophobic contacts while AR1–3 contacts helix 3 (residues 289–300), *via* mainly electrostatic contacts (Fig. 1c).[10] Meanwhile, AR3–6 and the first part of the IκBα PEST sequence contact the NFκB p50 and RelA dimerization domains and RelA amino-terminal domain.[10,17] In contrast to the observed electron

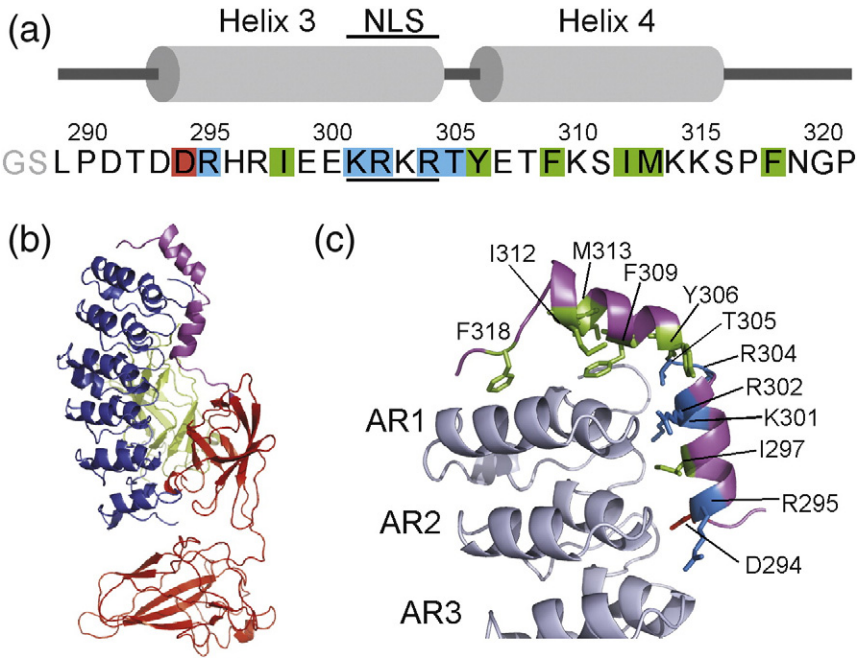

Fig. 1. (a) The sequence of the RelA NLS polypeptide showing interactions with IκBα is shown below a schematic of the secondary structure of the RelA NLS from the x-ray crystal structure.[10] Boxes indicate residues involved in interaction with IκBα: green, hydrophobic interaction; red and blue, electrostatic interaction. The residues of the putative NLS, KRKR, are underlined and their position at the end of helix 3 is indicated. (b) Ribbon diagram showing the x-ray crystal structure of the NFκB–IκBα complex.[10] The p50 subunit is colored in green, the RelA DNA-binding and dimerization domains in red, and the RelA NLS polypeptide in magenta. IκBα is colored in blue. (c) Ribbon diagram showing the interactions between the RelA NLS polypeptide (magenta) and IκBα (grey). Residues making interactions are colored according to the boxes in part (a).

density for the RelA NLS polypeptide when bound to IκBα, no density is observed for this region of NFκB (RelA/p50) bound to DNA, suggesting that the RelA NLS is disordered and available for importin-α binding until the NFκB binds to IκBα.[10,18] In addition, the apparent disorder of the free RelA NLS suggests inherent flexibility that may facilitate adoption of different local structures in order to bind multiple targets, such as IκBα and importin α.[19] In fact, NLSs bound to importin α usually adopt extended structures, while the RelA NLS polypeptide adopts a split helical conformation (termed helix3-helix4) when bound to IκBα.[10,20]

Thermodynamic and kinetic studies of the NFκB (RelA/p50)–IκBα interaction revealed that the interaction has an extremely low dissociation rate and a concomitantly high affinity, consistent with the long lifetime of the complex *in vivo*.[21] This study also showed that the NFκB(RelA/p50)–IκBα interaction depends critically on the RelA NLS, since truncating helix 4 of RelA resulted in a more than 1000-fold increase in the dissociation rate and a 10,000-fold decrease in the affinity of IκBα for NFκB(RelA/p50) and contributed more significantly to the ΔCp_{obs} and ΔG_{obs} than one would expect from such a small deletion.[21] In the present study, we have employed NMR and isothermal titration calorimetry (ITC) in order to characterize the structural and dynamic changes in the RelA NLS polypeptide in the free and IκBα-bound states in solution. The NMR studies presented here show that the RelA NLS is disordered in the free state and folds upon binding to IκBα. In addition, mutagenesis reveals that a single residue is critically important for high affinity.

Results

The minimal NLS and NLS–IκBα complex

Residues 289–321 of RelA are traditionally identified as the NLS peptide, although only the KRKR (residues 301–304) technically comprise the NLS. Heteronuclear single quantum coherence (HSQC) spectra of the peptide corresponding to RelA(289–321) showed missing peaks and uneven peak intensities that were localized to the flexible linker (residues 289–292) between the dimerization domain and helix 3 of the NLS. We therefore show only NMR spectra from the peptide corresponding to RelA (293–321), as it yielded a greater number of peaks of more even peak intensity in the complex even though the results presented here were obtained for both sequences. To form the minimal complex, a truncated form of IκBα, which contains only the first four ankyrin repeats of IκBα (residues 67–206),[22] was used because in the crystal structure of the NFκB–IκBα complex, the NLS polypeptide interacts only with the first three ankyrin repeats of IκBα. This minimal complex had significantly improved solubility characteristics for NMR study.[22]

Backbone resonance assignments

The HSQC spectra of free and IκBα-bound RelA (293–321) are compared in Fig. 2. Backbone resonance assignments of ^{15}N, ^{13}C-labeled RelA (293–321), free and in complex with IκBα(67–206), were obtained using standard triple resonance methods. Additional minor cross-peaks were observed for residues 309–315, which we attribute to the possible presence of a small population of molecules containing an oxidized methionine at position 313. The HSQC spectra clearly show that in the free form, the NLS polypeptide is unstructured, whereas a marked increase in resonance dispersion, consistent with the formation of a folded structure, is observed for the IκBα-bound state (Fig. 2).

Secondary structure of free and bound RelA NLS in solution

Secondary chemical shifts calculated from the difference between the observed and sequence-corrected random-coil chemical shifts[23] are shown for ^{15}N, $^{13}C_\alpha$, $^{13}C_\beta$, and ^{13}CO resonances of free and IκBα(67–206)-bound RelA(293–321) in Fig. 3. Positive values of $^{13}C_\alpha$, $^{13}C_\alpha$–$^{13}C_\beta$, and ^{13}CO and negative ^{15}N values show the presence of a helical structure in bound RelA(293–321) (Fig. 3b); residues 304–305, which are in a turn between helix 3 and helix 4 in the crystal structure of the IκBα–NFκB complex, show reduced secondary chemical shift

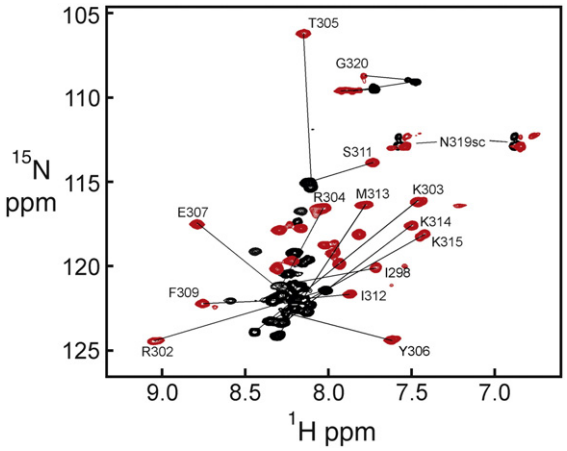

Fig. 2. Superposition of ^{1}H-^{15}N HSQC spectrum of 0.2 mM ^{1}H-^{15}N-RelA NLS(293–321) (black) with ^{1}H-^{15}N HSQC spectrum of ^{2}H-^{15}N-RelA NLS(293–321) (0.4 mM)/^{2}H-IκBα(67–206) (0.6 mM) (red), showing selected assignments. Both spectra were collected at 600 MHz and 293 K.

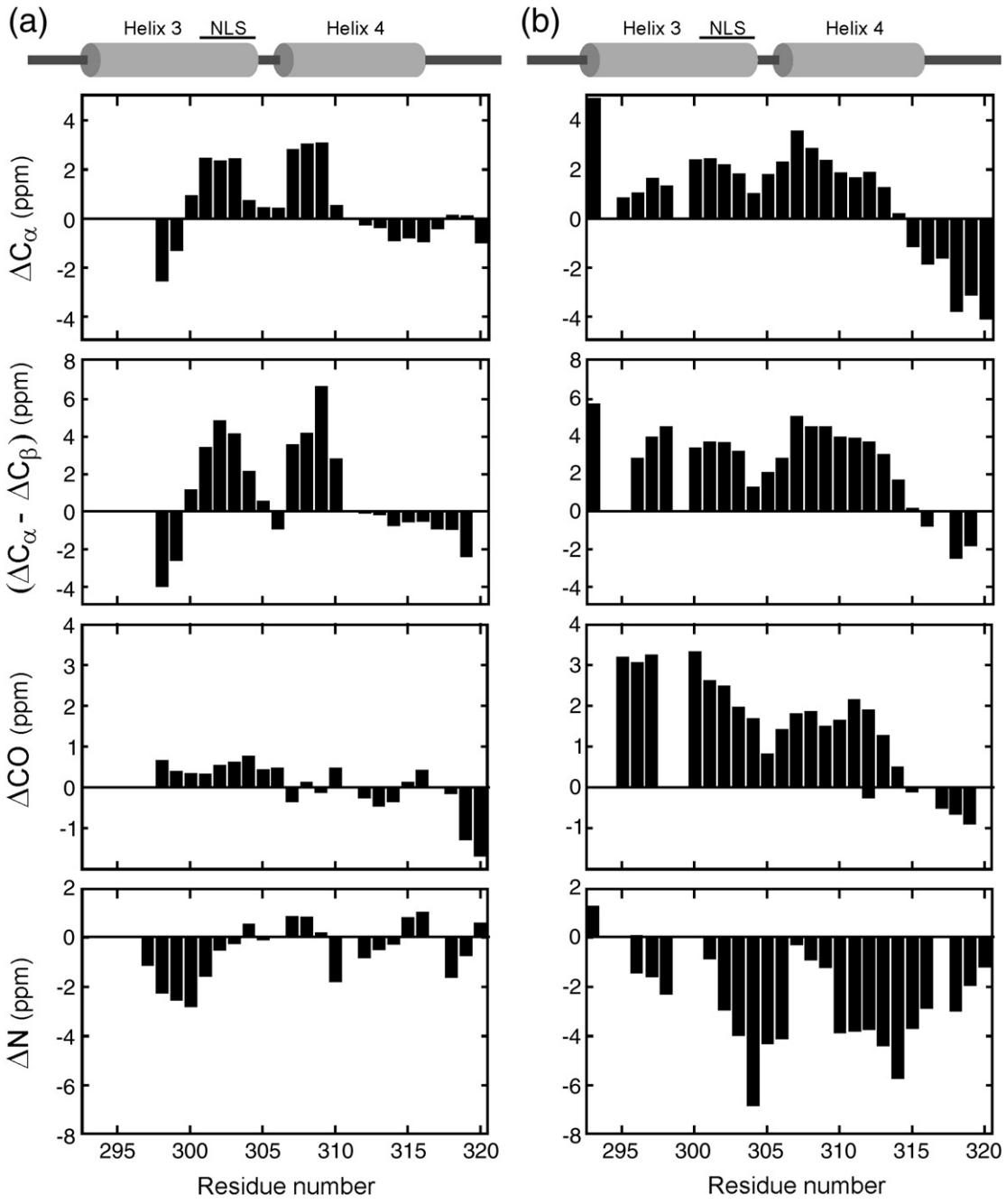

Fig. 3. Secondary chemical shifts of (a) free and (b) IκBα(67–206)-bound RelA NLS. Cross-peaks for residues 293–296 of the free peptide and residues 294–295 and 296–297 for the bound peptide were missing and these residues could not be assigned. Differences (in ppm) of observed *versus* sequence-corrected random-coil values for C_α, C_α–C_β, CO, and N chemical shifts are shown. A schematic of the secondary structure of the RelA NLS from the x-ray crystal structure is shown at the top of each column.

values.[10] Negative values of $^{13}C_\alpha$, $^{13}C_\alpha$–$^{13}C_\beta$, and ^{13}CO were observed for the C-terminal residues 315–320, consistent with the lack of secondary structure seen in the crystal structure[10] for this region.

The lower values of the secondary ^{15}N, $^{13}C_\alpha$, $^{13}C_\alpha$–$^{13}C_\beta$, and ^{13}CO chemical shifts for free RelA NLS(293–321) (Fig. 3a) were indicative of an unfolded peptide, but it clearly has residual helical structure with helix 3 having a slightly greater helical propensity than helix 4. The slight helical tendency was also more pronounced in data collected at 278 K.

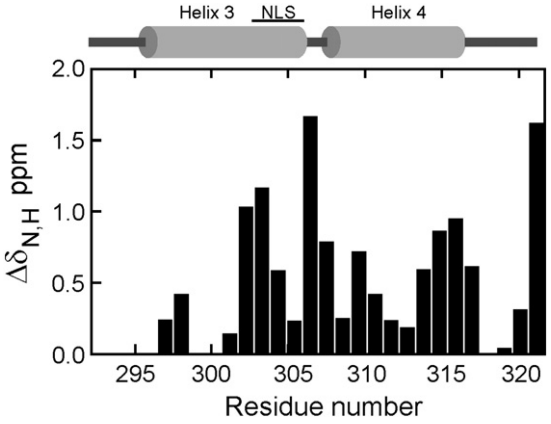

Fig. 4. Chemical-shift differences between free and IκBα(67–206)-bound ^{15}N-RelA NLS(293–321), calculated from chemical shifts measured in ^{1}H-^{15}N HSQC spectra obtained at 800 MHz and 293 K according to the formula $\Delta\delta = [(\Delta\delta_{HN})^2 + (0.1\ \Delta\delta_N)^2]^{1/2}$. A schematic of the secondary structure of the RelA NLS from the x-ray crystal structure is shown at the top of the figure.

Chemical shift perturbation

The differences in the chemical shifts between free and IκBα(67–206)-bound RelA NLS(293–321) are shown in Fig. 4. The largest changes correspond to residues located in the turn between helix 3 and helix 4 and at the C-terminal ends of helix 3 (the NLS region) and helix 4 (residues 313–316). Large changes were also seen in Gly320 for which multiple peaks were observed, possibly from conformational exchange due to its proximity to the C terminus.

The resonances of IκBα(67–206) are also perturbed upon binding of RelA(293–321) (Fig. 5). The most extreme chemical shift changes in IκBα(67–206) were observed for residues that form contacts with the RelA NLS as seen in the crystal structure of the complex, indicating that binding of the isolated NLS polypeptide is the same as occurs when it is part of the RelA protein.

Backbone dynamics

Internal motions on a picosecond–nanosecond timescale were estimated by measuring the ^{15}N-^{1}H heteronuclear nuclear Overhauser enhancement (NOE) for free and IκBα(67–206)-bound RelA NLS(293–321). Heteronuclear NOE measurements were also collected for free RelA NLS(289–321) at 278 K. The heteronuclear NOE values of the bound NLS ranged from 0.8 to 1, indicative of a well-structured peptide, except at the ends where values decrease below 0.5 (Fig. 6a). Heteronuclear NOE values for RelA NLS(289–321) at 278 K are higher than those for RelA NLS(293–321) at 293 K but lower than those seen for the complex. Slightly lower heteronuclear NOE values were measured for helix 4 in comparison to helix 3 at 278K. The heteronuclear NOEs for the free RelA NLS(293–321) were below 0.7, characteristic of a disordered protein.

Hydrogen exchange probed by CLEANEX-PM experiments

Further information on the conformational ensemble of free RelA NLS(293–321) was provided by amide-exchange measurements made using the CLEANEX-PM method.[24] This experiment is useful for probing nascent structure in intrinsically disordered proteins.[25] In general, the intensity of the cross-peaks increased with CLEANEX mixing time, indicating efficient exchange with the solvent, as expected for an unfolded peptide, but differences were observed between various parts of the sequence (Fig. 6b). The bend between the two helices (residues 305–307) showed the highest exchange rates. These residues also had lower heteronuclear NOEs (Fig. 6a) and chemical shift values that were closer to random-coil values (Fig. 3a). Residues 302–304, 308–312, and 318 show

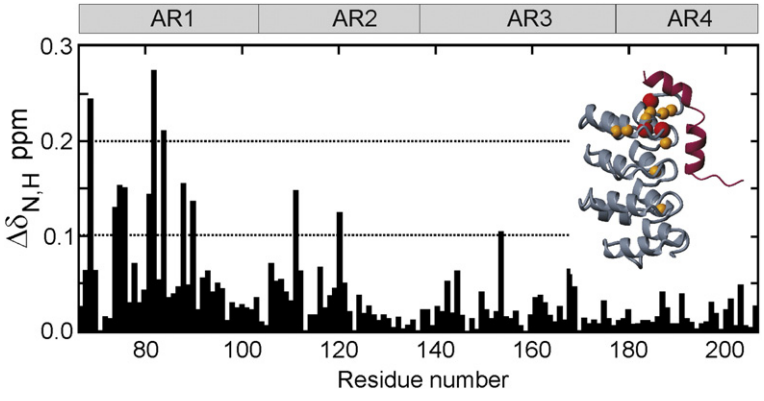

Fig. 5. Chemical-shift differences between free and RelA-NLS-bound ^{15}N-IκBα(67–206) were calculated from chemical shifts measured in ^{1}H-^{15}N HSQC spectra taken at 800 MHz and 298 K and calculated in the same manner as in Fig. 4. Inset: position of the amide N of residues with highest chemical-shift differences between free and bound ^{15}N- IκBα(67–206), shown as spheres on the structure of IκBα(67–206) from the NFκB–IκBα complex.

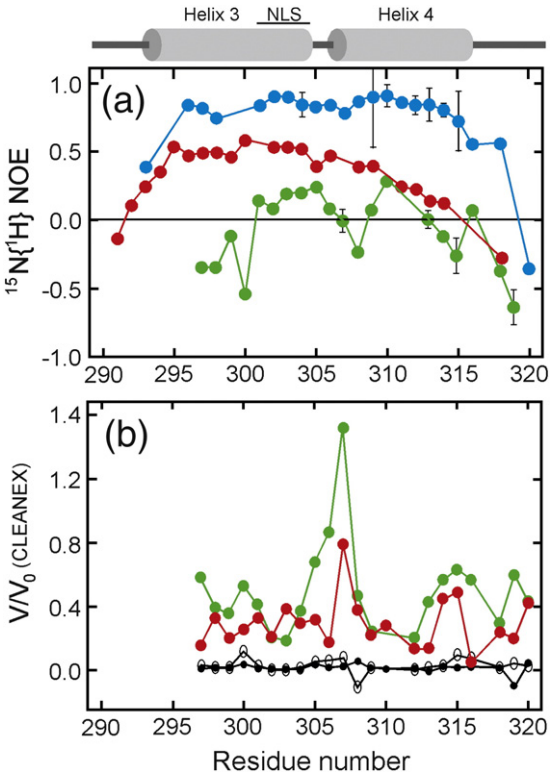

Fig. 6. (a) ^{15}N-^{1}H Heteronuclear NOE values for free and IκBα(67–206)-bound RelA NLS. Blue: ^{2}H-^{15}N-RelA NLS(293–321) (0.4 mM)/^{2}H-IκBα(67–206) (0.6 mM) [600 MHz, 293 K]; red: ^{15}N-RelA NLS(289–321) (1 mM) [500 MHz, 278 K]; green: ^{15}N-RelA(293–321) (0.3 mM) [293 K, 600 MHz]. Error bars represent the deviation between two independent experiments. (b) Ratio of cross-peak intensities between a CLEANEX-PM[24] spectrum recorded with zero mixing time and those at 2 ms (open circles) and 100 ms (filled circles). All spectra were collected on a 0.3 mM ^{15}N-RelA NLS(293–321) sample at 501 MHz at 278 K (red) and 293 K (green).

lower CLEANEX ratios and higher heteronuclear NOEs, indicating relatively more nascent helical structure.

Alanine scanning mutagenesis identifies critical binding residues in the NLS

Previous experiments identified helix 4 as a hot spot for the NFκB–IκBα interaction; this helix alone contributes some 7.8 kcal/mol to IκBα binding.[21] To pinpoint the residues that contribute most to the binding affinity, the contact residues of the RelA NLS helix 4 identified from the crystal structure[10] were each mutated to alanine. The results of these experiments are summarized in Table 1 and Fig. 7. None of the mutations had a significant effect on the binding affinity of RelA (289–321) to IκBα(67–206) except for the F309A mutation, which dramatically decreased binding to an unmeasurable value (Fig. 7). In order to quantify the importance of F309 for binding in the context of NFκB as a whole, we introduced the F309A mutation in a construct co-expressing the heterodimer of the dimerization domains, RelA (190–321)/p50(248–350). Although the binding affinity of the wild-type proteins is too high for accurate estimation of the K_D by ITC, the F309A RelA(190–321)/p50(248–350) bound at least 30-fold more weakly to IκBα(67–287), as indicated by both K_D and ΔH (Table 1).

Binding isotherms were also obtained at 50 mM and 150 mM NaCl in order to probe the effect of electrostatic contacts, which appear from the crystal structure to mediate the binding of RelA NLS helix 3 to IκBα (Fig. 1). The effect of ionic strength was fairly small, causing a less than 2-fold difference in $K_{D,obs}$ for both RelA(293–321) and RelA(289–321) (Table 1).

We also measured the temperature dependence of the binding of RelA(289–321) to IκBα(67–287). The ΔH varied linearly with temperature, resulting in a ΔCp of −0.4 kcal M^{-1} K^{-1} (Supplementary Fig. S1). Unfortunately, the ΔH decreased to zero at around 20 °C, and we were unable to measure it with confidence at lower temperatures to look for the curvature indicative of coupled folding and binding that has been observed by others.[26]

Table 1. Binding thermodynamics of IκBα and RelA constructs measured by ITC

RelA NLS	Mutation	[NaCl] (mM)	K_D (nM)	ΔH (kcal mol^{-1})	$-T\Delta S$ (kcal mol^{-1})	ΔG (kcal mol^{-1})
293–321	(WT)	50	371 ± 1	−4.2 ± 0.2	−4.4 ± 0.2	−8.6 ± 0.3
293–321	(WT)	150	746 ± 16	−4.3 ± 0.2	−3.9 ± 0.2	−8.2 ± 0.3
289–321	(WT)	50	800 ± 64	−3.7 ± 0.03	−4.4 ± 0.1	−8.1 ± 0.1
289–321	(WT)	150	1160 ± 13	−3.6 ± 0.4	−4.4 ± 0.4	−8.0 ± 0.8
289–321	Y306A	50	2600 ± 40	−2.3 ± 0.01	−5.2 ± 0.1	−7.5 ± 0.1
289–321	F309A	50	ND	ND	ND	ND
289–321	I312A	50	540 ± 2	−7.3 ± 0.2	−1.1 ± 0.01	−8.4 ± 0.02
289–321	M313A	50	970 ± 50	−3.0 ± 0.02	−5.1 ± 0.04	−8.1 ± 0.1
289–321	F318A	50	2700 ± 700	−2.5 ± 0.01	−5.0 ± 0.2	−7.5 ± 0.2
190–321	(WT)	50	<1	−12	ND	ND
190–321	F309A	50	19	−8	−2	−10

ND, could not be determined.

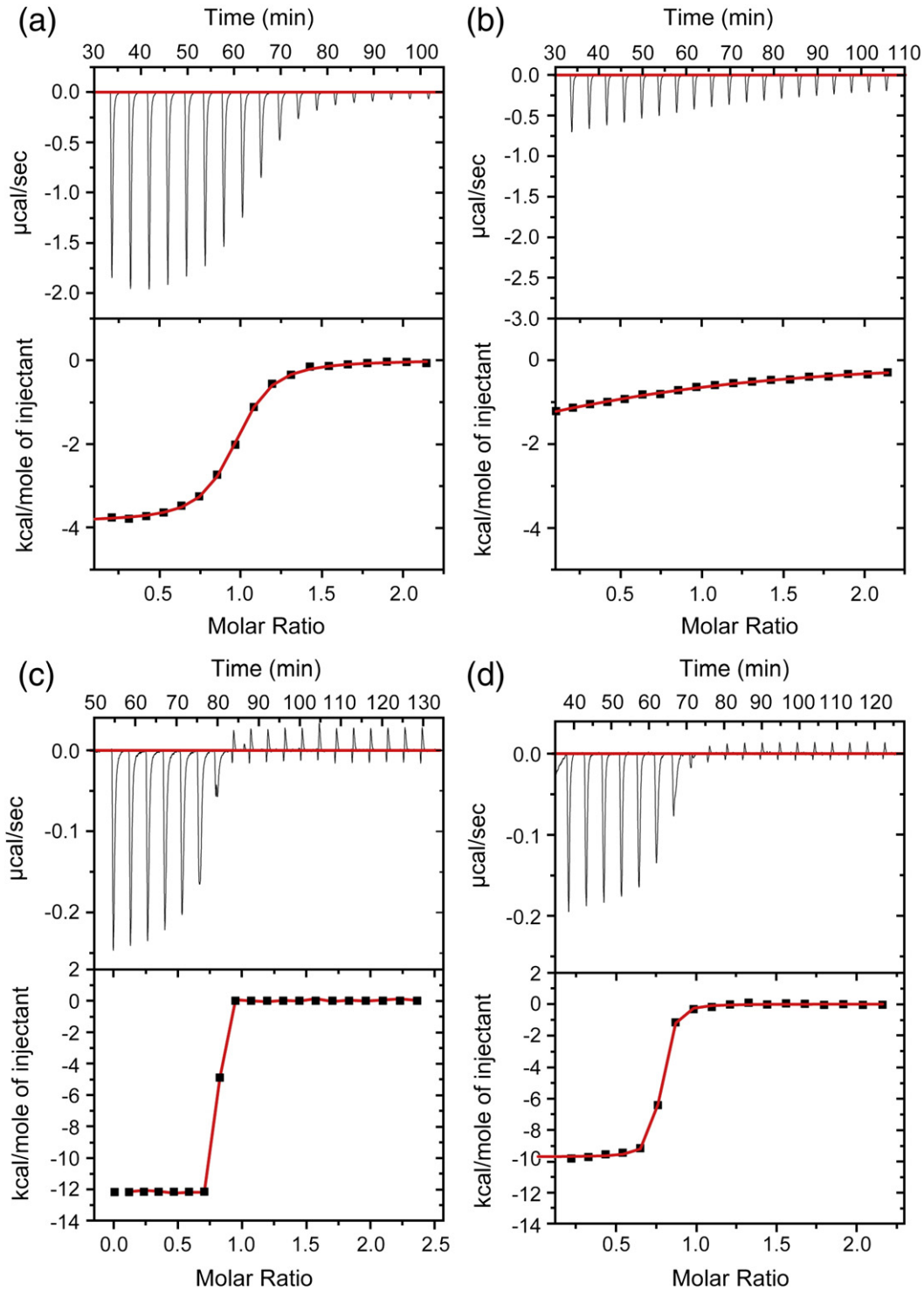

Fig. 7. ITC results for binding of (a) WT RelA NLS(293–321), (b) F309A RelA NLS(293–321), (c) WT RelA(190–321)/p50(248–350), and (d) F309A RelA(190–321)/p50(248–350) to IκBα(67–206) in 50 mM NaCl, 25 mM Tris (pH 7.5), 0.5 mM EDTA, and 0.5 mM sodium azide at 293 K. Data were analyzed using a model for a single set of identical binding sites after the heat of dilution of NFκB into buffer was subtracted. Thermodynamic values obtained from these curves are given in Table 1.

Discussion

The RelA NLS folds upon binding IκBα

IκBα binds and retains NFκB in the cytoplasm until the inhibition is relieved by degradation of IκBα following receipt of an extracellular signal. Because no electron density was observed for RelA residues 289–321 in the DNA-bound NFκB(RelA/p50) structure, the suggestion was made that the RelA NLS polypeptide might be unfolded in the absence of IκBα.[27] Prediction of disorder propensity using the IUPred algorithm[28] also suggests that the NLS polypeptide of RelA (residues 289–321) should be disordered. The X-ray structure of the IκBα–NFκB complex that included residues 305–321 of RelA showed two different molecules in the asymmetric unit, one with the NLS polypeptide sandwiched between the top of IκBα and the next molecule in the asymmetric unit and the other with the NLS polypeptide only half-bound.[10] Our results using NMR experiments to elucidate the structure and backbone dynamics and ITC experiments to elucidate the thermodynamics of the IκBα/RelA-NLS interaction provide the first direct experimental evidence that the NLS polypeptide folds upon binding IκBα. The NMR data show that the free form is clearly in a disordered, highly dynamic configuration, although residual helical propensity in a few regions is definitely observed. The bound form adopts a stable helical conformation with much more well-dispersed signals indicative of a unique fully folded and bound conformation. Reverse chemical shift perturbation allowed us to map the "footprint" of the NLS polypeptide onto the IκBα, and this "footprint" matches what would be expected from the crystallographically determined structure in complex with IκBα.[10] To further confirm whether the NLS polypeptide folds upon binding, we attempted to measure the temperature dependence of the ΔH observed during the binding reaction. A ΔCp of -0.4 kcal M^{-1} K^{-1} was measured. However, attempts to rationalize whether this was consistent with the expected surface area buried upon binding[29] were confounded by the fact that the NLS polypeptide was bound to differing extents in the two molecules in the asymmetric unit,[10] which yielded a range of predicted ΔCp values between -0.26 and -0.41 kcal M^{-1} K^{-1}.

Mutagenesis identifies residues critical for the IκBα–NFκB interaction

The contributions to binding of IκBα contacting residues within helix 4 of the NLS polypeptide, Tyr306, Phe309, Ile312, Met313, and Phe318, were examined by ITC, comparing the behavior of the wild-type protein with that of mutants where these residues were substituted with alanine. Most of the mutations caused only slight decreases in binding affinity of the RelA NLS for IκBα, but binding of the F309A mutant was virtually abolished. These studies therefore identify the hot spot[30] of this highly specific interaction as a single residue, Phe309, which appears in the crystal structure[10] to fit into a hydrophobic pocket on the top face of IκBα formed by Phe77 and Leu80. This is in accordance with the prediction that Phe309 would be crucial for binding of helix 4 to IκBα, as it formed several native and nonnative contacts with IκBα in folding and binding simulations.[31] In the present study, Phe309 emerges as a sort of anchor helping to clamp helix 4 to IκBα.

The I312A mutant demonstrates enthalpy–entropy compensation: ΔH of binding increases by 2-fold while $-T\Delta S$ decreases, thus achieving a similar binding affinity to that of the wild-type peptide. Both the entropy decrease and the enthalpy increase may be due to the substitution of a helix-disrupting β-branched side chain, which does not appear to be making any specific contacts in the bound structure, with alanine, which would promote helix formation. It is also interesting that mutation of Phe318, which appears to contact IκBα in the crystal structure[10] (Fig. 1c), had little effect on the binding affinity. This difference may identify the area around Phe318 as strongly influenced by crystal contacts into a conformation that is not characteristic of the complex in solution.

Significance of the NLS–IκBα interaction

The folding of the RelA NLS polypeptide upon binding to AR1–3 of IκBα explains the mechanism whereby IκBα-bound NFκB is retained in the cytoplasm. Although the crystal structure of the NFκB(RelA/p50)–IκBα complex hinted at the fact that the NLS was bound in a folded conformation on the surface of IκBα and therefore not accessible to importin α, the crystallographic *B*-factors were extremely high, and the affinity of the binding was not known.[10] Our results provide definitive evidence that the NLS polypeptide undergoes a disorder-to-order conformational change in the presence of IκBα, effectively masking it from binding by importin α and inhibiting subsequent translocation to the nucleus. In addition, the helical structure induced by IκBα binding is incompatible with the extended structure required for importin-α interaction.

The tight binding affinity of the NFκB(RelA/p50)–IκBα complex is encoded in two interactions, one at either end of the large protein–protein interface.[21,32] The interaction at the C-terminal part of IκBα involves the weakly folded fifth and sixth ankyrin repeats of IκBα that fold upon binding the N-terminal part of NFκB.[33] We demonstrate that at

the opposite end of the interface, the C-terminal NLS polypeptide of RelA also folds upon binding IκBα. Thus, the interaction may be said to follow a mutually synergistic "I-fold-you, you-fold-me" mechanism. Although both helix 3 and helix 4 of the NLS polypeptide fold upon binding to IκBα, it is helix 4, that is critical for the interaction.[21] Indeed, a single residue within helix 4, Phe309, is all-important for the binding affinity. We may visualize the Phe309 ring acting as a "button," fixing helix 4 to the "buttonhole" formed in the top face of the ARD of IκBα by Phe77 and Leu80. This highly specific interaction effectively caps the ankyrin repeat domain[34] generating significant favorable binding energy.

Materials and Methods

Protein expression and purification

The C-terminal sequences 289–321 and 293–321 of the RelA subunit of NFκB were expressed in the trp leader vector, which contains a His_8-tag and thrombin cleavage sequence, and drives small peptides into inclusion bodies.[35] Expression of unlabeled, ^{15}N-labeled, ^{2}H, ^{15}N-labeled, ^{13}C, ^{15}N-labeled, and ^{2}H, ^{13}C, ^{15}N-labeled peptides was carried out in M9 minimal medium in H_2O or D_2O supplemented with $^{15}NH_4Cl$ (2 g/L) and ^{13}C-glucose (8 g/L) as needed. Cells were acclimated by growing them sequentially in 10-mL cultures of M9ZB, M9, M9 (50% D_2O), and M9 (90% D_2O). Three 1-liter growths were inoculated with the M9 (90% D_2O) culture and induced at OD_{600} = 1.0 with 0.5 mM IPTG for 12 h at 37 °C. The cells were collected by centrifugation at 5000 rpm for 30 min. Inclusion bodies were solubilized with 6 M guanidine hydrochloride, 50 mM Tris (pH 7.5), and the solubilized peptide was captured by a Ni-NTA column equilibrated in the same buffer. A gradient was run to a final concentration of 150 mM NaCl, 50 mM Tris (pH 7.5), 2 mM $CaCl_2$. The peptide was cleaved from the column-bound fusion protein by incubating with thrombin (0.04 mg) in 3 column volumes by rocking the column for 4 h at 25 °C three consecutive times. The final purification step was reverse-phase HPLC on a C18 column (15 μm, 300 × 19 mm I.D.) with a 0–50% acetonitrile gradient, with 0.1% trifluoroacetic acid. The peptide was lyophilized and dissolved in 25 mM Tris (pH 7.5), 0.5 mM EDTA (ethylenediaminetetraacetic acid), 50 mM NaCl, and the pH adjusted with 10 M NaOH in 25 mM Tris, 0.5 mM EDTA, and 50 mM NaCl. The masses of all final purified peptides were verified by matrix-assisted laser desorption/ionization and electrospray ionization mass spectrometry. To study the binding of the NLS polypeptides to IκBα(67–206) by NMR, both the NLS polypeptide and the IκBα(67–206) were deuterated to minimize exchange broadening.

To monitor chemical shift perturbation of the IκBα(67-206) chemical shifts upon titration with unlabeled NLS 289–321, ^{15}N-labeled IκBα(67–206) was prepared as previously described.[22] For NMR studies of the complexes of labeled NLS polypeptides with IκBα(67–206), ^{2}H-labeled IκBα(67–206) was prepared in M9 minimal medium in D_2O. Cells were acclimated by growing them sequentially in 10-mL cultures of M9ZB, M9, M9 (50% D_2O), and M9 (90% D_2O). Two 1-liter growths were inoculated with the M9(90% D_2O) culture and induced at OD_{600} = 0.6 with 0.2 mM IPTG for 24 h at 18 °C. For all IκBα(67–206) preparations, the cells were collected by centrifugation at 5000 rpm for 30 min and resuspended in 70 mL/liter of culture of 25 mM Tris (pH 7.5), 50 mM NaCl, 0.5 mM EDTA, 10 mM β-mercaptoethanol, 0.3 mM PMSF, and protease inhibitor cocktail (Sigma) and lysed by sonication on ice. The soluble part of the lysate was purified by cation exchange chromatography on a Hi-Load Q-Sepharose 26/10 column (GE Healthcare) using a 1-h gradient from 50 to 500 mM NaCl. Final purification of the protein was done on a Superdex 75 16/60 gel filtration column (GE Healthcare). Final purification of the protein was done on a HiLoad Superdex 75 16/60 gel filtration column (GE Healthcare). The purified protein was concentrated in 4-mL 10K-MWCO Amicon concentrators (Millipore) in a fixed-angle rotor at 4000 rpm at 15-min intervals to prevent aggregation.

NMR experiments and data analysis

The structural and dynamic properties of free and bound RelA NLS were studied by NMR. NMR experiments for sequence-specific resonance assignment of RelA NLS(298–321) and (293–321) were carried out at 293 K to obtain sequence-specific assignment of H^N, N, C′, C^α, and C^β resonances for free and IκBα(67–206)-bound RelA NLS. A combination of HN(CA)CO, HNCO, and HNCACB was collected for free RelA NLS(293–321) and HNCA, HNCB, HNCO, and HN(CO)CACB for free RelA NLS(289–321) and bound RelA NLS(289–321) and (293–321).[36–38] The details of how each experiment was performed are given in Supplementary Table S1. Spectra were processed with NMRpipe[39] and analyzed using NMRView.[40] Backbone resonance assignments of NLS constructs were determined by establishing connectivities using the HN(CA)CO and HNCO spectra and separately using HNCA, HNCB, and HN(CO)CACB in an iterative manner.

In order to probe the dynamics and structure of RelA NLS in its free and complexed forms, we also measured the ^{15}N-^{1}H heteronuclear NOE of free and bound RelA NLS(293–321) at 293 K. Saturated and unsaturated spectra were recorded in an interleaved manner. Hydrogen exchange in free and bound RelA NLS(293–321) at 293 K was measured by fHSQC-CLEANEX-PM experiments.[24] To further characterize the structural and dynamic features of free RelA NLS(289–321), backbone resonance assignment experiments, ^{15}N-^{1}H heteronuclear measurements, and fHSQC-CLEANEX-PM experiments were also performed at 278 K in order to slow down conformational exchange of the free peptide.

Experimental details are reported in Supplementary Table S1. Data were processed using NMRpipe[39] and analyzed using NMRView[40] and Curvefit.[41] The secondary-structure propensity from the chemical shifts was determined by the approach described in Ref. 42, with random-coil reference chemical shift values[43,44] corrected for primary sequence[23] and for deuterium isotope effects for the bound RelA NLS.[45]

Isothermal titration calorimetry

ITC experiments were carried out on a Microcal VP ITC instrument. IκBα(67–206) was purified by size-exclusion chromatography (S75 column) immediately before use. In a typical ITC experiment, 25 injections of 15 μl of 1 mM RelA NLS or 0.05 mM NFκB(RelA/p50) dimerization domains were made into either IκBα(67–206) (0.1 mM) or IκBα(67–287) (0.005 mM) in the cell. ITC experiments were carried out in a buffer of 25 mM Tris (pH 7.5), 0.5 mM EDTA, 50 mM NaCl, 1 mM TCEP, and 0.5 mM sodium azide at 293 K in duplicate. Isotherms were analyzed using the Origin software (Microcal) as described.[46] The temperature dependence of binding of RelA NLS(289–321) to IκBα(67–287) was measured in 150 mM NaCl, 10 mM Mops (pH 7.5), and 0.5 mM EDTA between 294 and 303 K.

Supplementary Data

Supplementary data associated with this article can be found, in the online version, at doi:10.1016/j.jmb.2010.10.055

References

1. Baldwin, A. S., Jr (1996). The NF-κB and IκB proteins: new discoveries and insights. *Annu. Rev. Immunol.* **14**, 649–683.
2. Ghosh, S., May, M. J. & Kopp, E. B. (1998). NF-κB and Rel proteins: evolutionarily conserved mediators of immune responses. *Annu. Rev. Immunol.* **16**, 225–260.
3. Gerondakis, S., Grossmann, M., Nakamura, Y., Pohl, T. & Grumont, R. (1999). Genetic approaches in mice to understand Rel/NF-κB and IκB function: transgenics and knockouts. *Oncogene*, **18**, 6888–6895.
4. Pahl, H. L. (1999). Activators and target genes of Rel/NF-κB transcription factors. *Oncogene*, **18**, 6853–6866.
5. Karin, M. & Ben-Neriah, Y. (2000). Phosphorylation meets ubiquitination: the control of NF-κB activity. *Annu. Rev. Immunol.* **18**, 621–663.
6. Huxford, T., Malek, S. & Ghosh, G. (1999). Structure and mechanism in NF-κB/IκB signaling. *Cold Spring Harb. Symp. Quant. Biol.* **64**, 533–540.
7. O'Dea, E. L., Barken, D., Peralta, R. Q., Tran, K. T., Werner, S. L., Kearns, J. D. *et al.* (2007). A homeostatic model of IκB metabolism to control constitutive NF-κB activity. *Mol. Syst. Biol.* **3**, 111.
8. Tergaonkar, V., Correa, R. G., Ikawa, M. & Verma, I. M. (2005). Distinct roles of IκB proteins in regulating constitutive NF-κB activity. *Nat. Cell. Biol.* **7**, 921–923.
9. Baeuerle, P. A. & Baltimore, D. (1988). IκB: a specific inhibitor of the NF-κB transcription factor. *Science*, **242**, 540–546.
10. Jacobs, M. D. & Harrison, S. C. (1998). Structure of an IκBα/NF-κB complex. *Cell*, **95**, 749–758.
11. Dang, C. V. & Lee, W. M. (1988). Identification of the human c-myc protein nuclear translocation signal. *Mol. Cell. Biol.* **8**, 4048–4054.
12. Dingwall, C. & Laskey, R. A. (1991). Nuclear targeting sequences—a consensus? *Trends Biochem. Sci.* **16**, 478–481.
13. Kalderon, D., Richardson, W. D., Markham, A. F. & Smith, A. E. (1984). Sequence requirements for nuclear location of simian virus 40 large-T antigen. *Nature*, **311**, 33–38.
14. Lanford, R. E. & Butel, J. S. (1984). Construction and characterization of an SV40 mutant defective in nuclear transport of T antigen. *Cell*, **37**, 801–813.
15. Leung, S. W., Harreman, M. T., Hodel, M. R., Hodel, A. E. & Corbett, A. H. (2003). Dissection of the karyopherin α nuclear localization signal (NLS)-binding groove: functional requirements for NLS binding. *J. Biol. Chem.* **278**, 41947–41953.
16. Malek, S., Huxford, T. & Ghosh, G. (1998). IκBα functions through direct contacts with the nuclear localization signals and the DNA binding sequences of NF-κB. *J. Biol. Chem.* **273**, 25427–25435.
17. Huxford, T., Huang, D. B., Malek, S. & Ghosh, G. (1998). The crystal structure of the IκBα/NF-κB complex reveals mechanisms of NF-κB inactivation. *Cell*, **95**, 759–770.
18. Huang, D. B., Huxford, T., Chen, Y. Q. & Ghosh, G. (1997). The role of DNA in the mechanism of NFκB dimer formation: crystal structures of the dimerization domains of the p50 and p65 subunits. *Structure*, **5**, 1427–1436.
19. Dyson, H. J. & Wright, P. E. (2002). Coupling of folding and binding for unstructured proteins. *Curr. Opin. Struct. Biol.* **12**, 54–60.
20. Conti, E. & Kuriyan, J. (2000). Crystallographic analysis of the specific yet versatile recognition of distinct nuclear localization signals by karyopherin α. *Structure*, **8**, 329–338.
21. Bergqvist, S., Croy, C. H., Kjaergaard, M., Huxford, T., Ghosh, G. & Komives, E. A. (2006). Thermodynamics reveal that helix four in the NLS of NF-κB p65 anchors IκBα, forming a very stable complex. *J. Mol. Biol.* **360**, 421–434.
22. Cervantes, C. F., Markwick, P. R. L., Sue, S. C., McCammon, J. A., Dyson, H. J. & Komives, E. A. (2009). Functional dynamics of the folded ankyrin repeats of IκBα revealed by nuclear magnetic resonance. *Biochemistry*, **48**, 8023–8031.
23. Schwarzinger, S., Kroon, G. J., Foss, T. R., Chung, J., Wright, P. E. & Dyson, H. J. (2001). Sequence-dependent correction of random coil NMR chemical shifts. *J. Am. Chem. Soc.* **123**, 2970–2978.
24. Hwang, T., Mori, S., Shaka, A. J. & van Zijl, P. C. M. (1997). Application of phase-modulated CLEAN Chemical EXchange Spectroscopy (CLEANEX-PM) to detect water–protein proton exchange and intermolecular NOEs. *J. Am. Chem. Soc.* **119**, 6203–6204.
25. Csizmók, V., Felli, I. C., Tompa, P., Banci, L. & Bertini, I. (2008). Structural and dynamic characterization of intrinsically disordered human securin by NMR spectroscopy. *J. Am. Chem. Soc.* **130**, 16873–16879.
26. Cliff, M. J., Williams, M. A., Brooke-Smith, J., Barford, D. & Ladbury, J. E. (2005). Molecular recognition *via* coupled folding and binding in a TPR domain. *J. Mol. Biol.* **346**, 717–732.
27. Chen, F. E., Huang, D. B., Chen, Y. Q. & Ghosh, G. (1998). Crystal structure of p50/p65 heterodimer of transcription factor NF-κB bound to DNA. *Nature*, **391**, 410–413.

28. Dosztányi, Z., Csizmók, V., Tompa, P. & Simon, I. (2005). IUPred: web server for the prediction of intrinsically unstructured regions of proteins based on estimated energy content. *Bioinformatics*, **21**, 3433–3434.
29. Spolar, R. S. & Record, J. M. T. (1994). Coupling of local folding to site-specific binding of proteins to DNA. *Science*, **263**, 777–784.
30. Wells, J. A. (1996). Binding in the growth hormone receptor complex. *Proc. Natl Acad. Sci. USA*, **93**, 1–6.
31. Latzer, J., Papoian, G. A., Prentiss, M. C., Komives, E. A. & Wolynes, P. G. (2007). Induced fit, folding, and recognition of the NF-κB-nuclear localization signals by IκBα and IκBβ. *J. Mol. Biol.* **367**, 262–274.
32. Bergqvist, S., Ghosh, G. & Komives, E. A. (2008). The IκBα/NF-κB complex has two hot-spots, one at either end of the interface. *Protein Sci.* **17**, *2051–2058.*
33. Truhlar, S. M., Torpey, J. W. & Komives, E. A. (2006). Regions of IκBα that are critical for its inhibition of NF-κB.DNA interaction fold upon binding to NF-κB. *Proc. Natl Acad. Sci. USA*, **103**, 18951–18956.
34. Barrick, D., Ferreiro, D. U. & Komives, E. A. (2008). Folding landscapes of ankyrin repeat proteins: experiments meet theory. *Curr. Opin. Struct. Biol.* **18**, 27–34.
35. Guttman, M., Prieto, J. H., Handel, T. M., Domaille, P. J. & Komives, E. A. (2010). Structure of the minimal interface between ApoE and LRP. *J. Mol. Biol.* **398**, 306–319.
36. Grzesiek, S. & Bax, A. (1992). Improved 3D triple-resonance NMR techniques applied to a 31 kDa protein. *J. Magn. Reson.* **96**, 432–440.
37. Wittekind, M. & Mueller, L. (1993). HNCACB, a high-sensitivity 3D NMR experiment to correlate amide-proton and nitrogen resonances with the α- and β-carbon resonances in proteins. *J. Magn. Reson.* **101**, 201–205.
38. Yamazaki, T., Lee, W., Arrowsmith, C. H., Muhandiram, D. R. & Kay, L. E. (1994). A suite of triple-resonance NMR experiments for the backbone assignmnet of ^{15}N, ^{13}C, ^{2}H labeled proteins with high sensitivity. *J. Am. Chem. Soc.* **116**, 11655–11666.
39. Delaglio, F., Grzesiek, S., Vuister, G. W., Zhu, G., Pfeifer, J. & Bax, A. (1995). NMRPipe: a multidimensional spectral processing system based on UNIX pipes. *J. Biomol. NMR*, **6**, 277–293.
40. Johnson, B. A. (2004). Using NMRView to visualize and analyze the NMR spectra of macromolecules. *Methods Mol. Biol.* **278**, 313–352.
41. Mandel, A. M., Akke, M. & Palmer, A. G., III (1995). Backbone dynamics of Escherichia coli ribonuclease HI: correlations with structure and function in an active enzyme. *J. Mol. Biol.* **246**, 144–163.
42. Berjanskii, M. V., Neal, S. & Wishart, D. S. (2006). PREDITOR: a web server for predicting protein torsion angle restraints. *Nucleic Acids Res.* **34**, W63–W69.
43. Wishart, D. S., Bigam, C. G., Holm, A., Hodges, R. S. & Sykes, B. D. (1995). ^{1}H, ^{13}C and ^{15}N random coil NMR chemical shifts of the common amino acids. I. Investigations of nearest-neighbor effects. *J. Biomol. NMR*, **5**, 67–81.
44. Metzler, W. J., Constantine, K. L., Friedrichs, M. S., Bell, A. J., Ernst, E. G., Lavoie, T. B. & Mueller, L. (1993). Characterization of the three-dimensional solution structure of human profilin: ^{1}H, ^{13}C, and ^{15}N NMR assignments and global folding pattern. *Biochemistry*, **32**, 13818–13829.
45. Gardner, K. H., Rosen, M. K. & Kay, L. E. (1997). Global folds of highly deuterated, methyl-protonated proteins by multidimensional NMR. *Biochemistry*, **36**, 1389–1401.
46. Wiseman, T., Williston, S., Brandts, J. F. & Lin, L. N. (1989). Rapid measurement of binding constants and heats of binding using a new titration calorimeter. *Anal. Biochem.* **179**, 131–137.